Transdisciplinary Engineering: Crossing Boundaries
M. Borsato et al. (Eds.)

doi:10.3233/978-1-61499-703-0-563

Stochastic Analysis of the Kinematic Performance of a Planar 5R Symmetrical Parallel Mechanism

Fabian Andres LARA-MOLINA[1], Edson Hideki KOROISHI and Victor BOLZON
Federal University of Technology - Paraná, Department of Mechanical Engineering, Av. Alberto Carazzai 1640, Cornélio Procópio-PR, Brazil

Abstract. This paper aims at studying the kinematic model of the 5R symmetrical parallel mechanism considering the uncertainties in the lengths of links and the clearances in the active joints. The complete kinematic model of the 5R parallel mechanism is formulated in the presence of the uncertain parameters that are model as random variables. The stochastic analysis, based on the Monte Carlo Method, permits to evaluate numerically the performance of the mechanism when the uncertain parameters are considered. Thus, the kinematic model for several poses within the workspace is evaluated. Moreover, the variability in the workspace produced by the uncertain parameters is also analyzed.

Keywords. Kinematics, Parallel Mechanism, Monte Carlo Method, Uncertainties

Introduction

Parallel mechanisms have active and passive joints. Active joints are attached to actuators that provide mechanical power for the motion. Passive joints are under-actuated. In most cases, the joints are subject to clearances that deteriorate the overall performance of the mechanism. Additionally, manufacturing and assembling tolerances introduces small variations in the geometry of the joints that also produce positioning error affecting the performance of the mechanism. In agreement with this is necessary to quantify the effect of these uncertainties in order to analyze how these uncertainties affects the performance of parallel mechanism [1].

Several works have studied this issue in robotic manipulators considering different approaches. The probabilistic theory has been previously used in order to study the effects of uncertain parameters on the performance of robot manipulators. By using this approach, the uncertainties are modeled as random variables or random fields. Consequently, the reliability associated with the tolerances of geometrical and dynamical parameters of the manipulator are studied [2,3]. Moreover, Polynomial Chaos Theory was applied to study the effect of uncertain inertia and payload on SCARA robot dynamics [5]. Nevertheless, as an alternative approach to analyze the uncertain parameters of robotic manipulators, the fuzzy theory has been applied to analyze the dynamic behavior of robotic manipulators [6].

[1] Corresponding Author. Federal University of Technology - Paraná, Department of Mechanical Engineering, Av. Alberto Carazzai 1640, Cornélio Procópio-PR, Brazil; E-mail: fabianmolina@utfpr.edu.br

This paper aims at analyze the kinematics of the 5R parallel mechanism subjected to uncertain length of the links and clearances of the active joints. In accordance with that, the forward/inverse kinematic model and the workspace were formulated as function of the aforementioned uncertain parameters. The uncertain parameters are modeled as random variables and they are introduced in the kinematic model of the mechanism. The Monte Carlo Simulation is the stochastic solver used in order to compute the numerical response of the kinematic model with the uncertain parameters. Finally, the numerical results are analyzed.

1. Kinematic Model

The 5R planar parallel mechanism has two active or actuated joints, three passive of free joints and four links. The geometry of the 5R symmetrical parallel mechanism is defined according to Fig. 1. The active joints are located at A_i and they are denoted as θ_i (for i = 1,2). The passive joints are located at the end of each link of the active joints Bi. The end effector of the mechanism is located at P that is defined by x and y Cartesian coordinates. Additionally, the fixed reference frame O is defined in the middle of A_1A_2, therefore the symmetry of the mechanism is defined by $OA_1 = OA_2$, $A_1B_1 = A_2B_2$ and $B_1P = B_2P$. Consequently, the geometry of the 5R symmetrical mechanism can be defined by $OA_i = \bar{r}_3\ (r_3)$, $A_iB_i = \bar{r}_1(r_1)$ and $B_iP = \bar{r}_2(r_2)$.

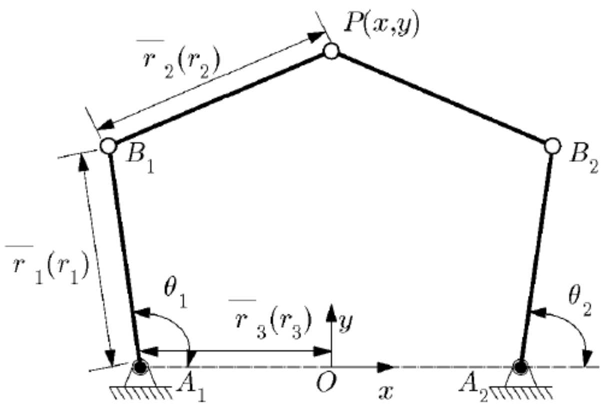

Figure 1. The 5R symmetrical parallel mechanism.

1.1. Inverse Kinematics

The inverse kinematic model defines the active joints θ_i as function of the position of end effector P. The position, P, of the end effector with respect of the fixed reference frame O is defined by the Cartesian vector $\mathbf{p} = (x, y)^T$. Additionally, the position of the points B_i (for i = 1,2) with respect to the fixed frame O is defined by the vector $\mathbf{b_1} = (r_1\cos(\theta_1) - r_3, r_1\sin(\theta_1))^T$ and $\mathbf{b_2} = (r_1\cos(\theta_2) + r_3, r_1\sin(\theta_2))^T$, respectively. The inverse kinematics is solved with the aids of the constraint equation $|\mathbf{b}_i\mathbf{p}| = r_2$, therefore:

$$(x - r_1 \cos(\theta_1) - r_3)^2 + (y - r_1 \sin(\theta_1))^2 = r_2^2 \quad (1)$$

$$(x - r_1 \cos(\theta_2) + r_3)^2 + (y - r_1 \sin(\theta_2))^2 = r_2^2 \quad (2)$$

by solving Eqs. (1) and (2) when **p** is known, θ_i can be determined:

$$\theta_i = \arctan(z_i) \quad (3)$$

where

$$z_i = \frac{-b_i + \sigma_i \sqrt{b_i^2 - 4a_i c_i}}{2a_i} \quad (4)$$

with

$\sigma_i = \pm 1$
$a_1 = r_1^2 + y^2 + (x + r_3)^2 - r_2^2 + 2(x + r_3)r_1$
$b_1 = -4yr_1$
$c_1 = r_1^2 + y^2 + (x + r_3)^2 - r_2^2 - 2\,(x + r_3)r_1$
$a_2 = r_1^2 + y^2 + (x - r_3)^2 - r_2^2 + 2\,(x - r_3)r_1$
$b_2 = b_1 = -4yr_1$
$c_2 = r_1^2 + y^2 + (x - r_3)^2 - r_2^2 + 2\,(x - r_3)r_1$

As seen in Eq. (4), the inverse kinematic has four different solutions that depend on the signal adopted by σ_i. The solution adopted in this paper considers $\sigma_1 = 1$ and $\sigma_2 = -1$. Based on Eqs. (3) and (4), the inverse kinematic can be expressed by the follow expression:

$$(\theta_1, \theta_2)^T = f(x, y, r_1, r_2, r_3) \quad (5)$$

1.2. Forward Kinematics

The forward kinematics model sets the position of end effector P as function of the active joints θ_i. It is obtained from Eqs. (1) and (2):

$$x^2 + y^2 - 2(r_1 \cos(\theta_1) - r_3)x - 2r_1 \sin(\theta_1)\, y - 2r_1 r_3 \cos(\theta_1) + r_3^2 + r_1^2 - r_2^2 \quad (6)$$

$$x^2 + y^2 - 2(r_1 \cos(\theta_2) + r_3)x - 2r_1 \sin(\theta_2)\, y + 2r_1 r_3 \cos(\theta_2) + r_3^2 + r_1^2 - r_2^2 \quad (7)$$

It is obtained from Eqs. (6) and (7):

$$x = ey + f \quad (8)$$

with $e = \frac{r_1(\cos(\theta_1) - \sin(\theta_1))}{2r_3 + r_1 \cos(\theta 2) - r_1 \cos(\theta 1)}$ and $f = \frac{r_1 r_3(\cos(\theta_1) + \cos(\theta_2))}{2r_3 + r_1 \cos(\theta_2) - r_1 \cos(\theta_1)}$. By substituting Eq.(8) to Eq. (6), it is obtained:

$$dy^2 + gy + h = 0 \quad (9)$$

with

$d = 1 + e^2$

$g = 2(ef - er_1 \cos(\theta_1) + er_3 - r_1 \sin(\theta_1))$

$h = f^2 - 2f(r_1\, cos(\theta_1) - r_3) - 2r_1 r_3\, cos(\theta_1) + r_3^2 + r_1^2 - r_2^2$

Considering Eq. 9,y can be obtained:

$$y = \frac{-g + \sigma\sqrt{g^2 - 4dh}}{2d} \tag{10}$$

From Eq. (10) is observed that the forward kinematic has two solutions corresponding to σ=1 or $\sigma = -1$. Based on Eqs. (8) and (10), the forward kinematic formulation can be summarized by the fallow expression:

$$(x, y)^T = f^{-1}(\theta_1, \theta_2, r_1, r_2, r_3) \tag{11}$$

1.3. Workspace of the Mechanism

The region of the workspace that the end effector can reach when the active joints θ_i variate from 0 to 2π is defined as the theoretical workspace, in this definition the collision between the links and the singularities are not considered. The theoretical workspace is enveloped by two following circles for the first leg:

$$C_{1o}: (x + r_3)^2 + y^2 = (r_1 + r_2)^2 \tag{12}$$

$$C_{1i}: (x + r_3)^2 + y^2 = (r_1 - r_2)^2 \tag{13}$$

For the second leg, the workspace is enveloped by circles:

$$C_{2o}: (x + r_3)^2 + y^2 = (r_1 + r_2)^2 \tag{14}$$

$$C_{2i}: (x + r_3)^2 + y^2 = (r_1 - r_2)^2 \tag{15}$$

The theoretical workspace is defined by the intersection of circles of Eqs. (12), (13), (14) and (15). The usable workspace is specified as the maximum continuous workspace that contains no singular loci, and also it is bounded outside by the singular loci. In the design process, the Maximum Inscribed Circle (MIC) is an index useful to evaluate the flatness of the usable workspace, the MIC is inscribed within the usable workspace and it is tangent with singular loci [4]. The Maximum Inscribed Workspace (MIW) is defined as the workspace bounded by the MIC. The MIC is characterized by the expressions:

$$x^2 + (y - y_{MIC})^2 = r_{MIC}^2 \tag{16}$$

where r_{MIC} is the radius and (0,y_{MIC}) is the center. For the cases when $r_1 + r_3 < r_2$, the MIC is defined by

$$r_{MIC} = \frac{r_1 + r_2 - |r_1 - r_2|}{2} \quad \text{and} \quad y_{MIC} = \sqrt{\frac{(r_1 + r_2 + |r_1 - r_2|)^2}{4} - r_3^2} \tag{17}$$

For the cases when $r_1 + r_3 > r_2$, the radius and center of the MIC are defined by:

$$r_{MIC} = |y_{MIC}| - y_{col} \qquad \text{and} \qquad y_{MIC} = \frac{(r_1+r_2+y_{col})^2 - r_3^2}{2(r_1+r_2+y_{col})} \tag{18}$$

with $y_{col} = \sqrt{r_1^2 - (r_2 - r_3)^r}$. Based of Eqs. (16), (17) and (18), the MIW can be expressed by using the follow expression:

$$[r_{MIW}\ y_{MIW}] = g(r_1, r_2, r_3) \tag{19}$$

where g is the the mathematical expression that computes r_{MIW} and y_{MIW} based on r_1, r_2 and r_3.

2. Stochastic Analysis

Typically the geometrical parameters of parallel robot are affected by uncertainties. Therefore, these uncertain parameters that consists in small variations around the nominal parameters introduce a variation in the solutions obtained of the kinematic model. Manufacturing tolerances include small variations in the geometrical parameters [7]. Consequently, the parameters selected in order to introduce the uncertainties in the kinematic model presented in the previous section are: the non-dimensional length of the links (r_1, r_2 and r_3), and clearances of the active joints: $\delta\theta_1$and $\delta\theta_2$).

The uncertain parameters are modeled as random variables. The corresponding uncertainties are introduced by using the follow relation:

$$a_0(\Omega) = a_0 + a_0\delta_a\xi(\Omega) \tag{20}$$

where $a_0$is the mean value of the parameter, δ_a is the dispersion level and $\xi(\Omega)$ is the unite normal random variable with Ω being a random process. The unite normal random variable is governed by a normal distribution, this distribution was selected in order to evaluate the uncertain parameters in this contribution.

The so-called Monte Carlo method combined with the Latin Hypercube sampling [8] is used to simulate the dynamic response of the robot with the considered uncertain random parameters. The Monte Carlo method combined with the Latin Hypercube permits to evaluate the uncertain response of a system by considering the fewer samples than using only Monte Carlo method. Additionally, with the aid of a convergence analysis helps determining the number of Monte Carlo samples ns to obtain an accurate result in the simulations.

3. Simulation Results

The uncertain parameters of the parallel mechanism for the inverse, forward kinematics and workspace are considered as random variables. These random variables are defined based on the Eq. (20). As it was stated previously the uncertainties in parallel mechanisms are associated with the manufacturing errors of links and the clearances of joints. The parameters of the non-dimensional length of the links (r_1, r_2 and r_3), and the clearances of the active joints ($\delta\theta_1$, $\delta\theta_2$) are defined in Table 1 in order to evaluate numerically the influence of these uncertain parameters on the kinematics. These uncertain values were selected based on previous contributions [1].

Table 1. Uncertain Parameters of the manipulator.

Parameter	$r_1(\Omega)$	$r_2(\Omega)$	$r_3(\Omega)$	$\delta\theta_1(\Omega)$	$\delta\theta_2(\Omega)$
a_0	1.2	1.0	0.8	0.25°	0.25°
δ_a	1%	1%	1%	100%	100%

The uncertain parameters of the manipulator are mapped on the kinematic model by using the Monte Carlo Simulation in order to evaluate the kinematics of mechanism in the presence of uncertainties. For this, $n_s = 150$ samples are used to compute the Monte Carlo Simulation.

3.1. Forward Kinematics

This analysis aims at evaluating the forward kinematics of the mechanism considering uncertainties in the non-dimensional lengths of the link and the clearances of the active joints that were previously described in Table 1. Consequently, the uncertainties were introduced in the forward kinematic model based on Eq. (21).

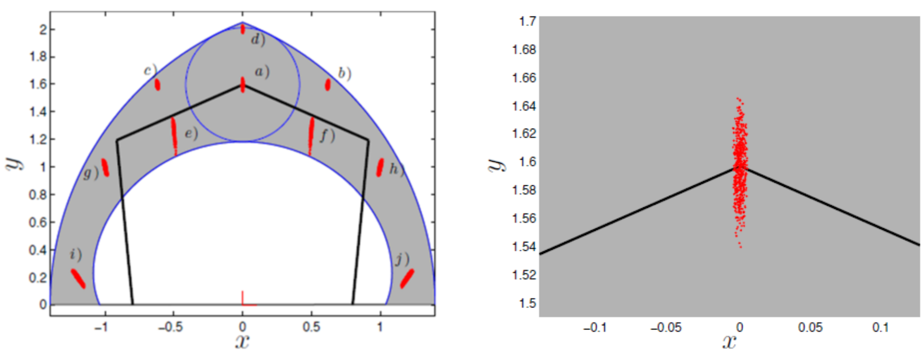

(a) (b)

Figure 2. Forward Kinematic solutions with uncertain parameters: (a) For all cases, (b) Zoom of case a).

$$\left(x(\Omega), y(\Omega)\right)^T = f^{-1}\left(\theta_1 + \delta\theta_1(\Omega), \theta_2 + \delta\theta_2(\Omega), r_1(\Omega), r_2(\Omega), r_3(\Omega)\right) \tag{21}$$

The forward kinematic with the uncertain parameters of Eq. (21) was evaluated for several poses (θ_i) within the usable workspace as presented in Fig. 2. Additionally, Fig. 2 shows the usable workspace and the MIW for $r_1 = 1.2$, $r_2 = 1.0$ and $r_3 = 0.8$.

Additionally, Table 2 presents the results of the forward kinematics which are mean and standard deviation the Cartesian position of the end effector in the x and y axis, $\bar{x}$, $\bar{y}$, σ_x, σ_y, respectively.

Table 2. Forward Kinematic with Uncertainties.

Case	θ_1	θ_2	$\bar{x}$	$\bar{y}$	σ_x	σ_y
a)	95.5181	84.4819	3.5586e-08	1.5966	0.0020	0.0193
b)	60.8802	58.0319	0.6200	1.5969	0.0040	0.0138
c)	121.9681	119.1198	-0.6200	1.5969	0.0040	0.0139
d)	78.8909	101.1091	-6.3229e-07	2.0000	0.0013	0.0110
e)	123.5349	104.7752	-0.4996	1.2648	0.0046	0.0439
f)	75.2248	56.4651	0.4996	1.2648	0.0048	0.0439
g)	154.1033	132.2085	-0.9998	0.9990	0.0071	0.0247
h)	47.7915	25.8967	0.9998	0.9990	0.0072	0.0245
i)	27.4773	-26.8307	1.1988	0.1982	0.0179	0.0260
j)	-153.1693	152.5227	-1.1988	0.1982	0.0177	0.0259

The results indicates that the uncertainties in the non-dimensional lengths of the links and the clearances of the active joints introduce a variability in the Cartesian position of the end effector of the mechanism, **p**, for all the cases considered in this analysis, this variability is quantified by the standard deviation σ_x and σ_y of each single pose. The variability in **p** is specially larger for the configurations closed to the singular loci singularities (cases: *e), f), i)* and *j)*). Additionally, it is observed that the poses closed to the limits of the usable workspace have a moderate variability with respect to the previous cases (cases: *c), g)* and *h)*). However, for the poses within the MIW, the forward kinematics exhibits a smaller variability (cases: *a)* and *d)*).

3.2. Inverse Kinematics

In this analysis the inverse kinematics is analyzed subject to uncertainties in the non-dimensional lengths of the link ($r_1(\Theta)$, $r_2(\Theta)$ and $r_3(\Theta)$) that were described in Table 1. The uncertainties were introduced in the inverse kinematic model based on Eq. (5), therefore, Eq. (22) describes the inverse kinematics with the uncertain parameters.

$$\left(\theta_1(\Omega), \theta_2(\Omega)\right)^T = f\left(x,\ y, r_1(\Omega), r_2(\Omega), r_3(\Omega)\right) \tag{22}$$

The inverse kinematic with the uncertain parameters of Eq. (22) was evaluated for the same poses that the forward kinematics was evaluated, i.e., for the poses described in Table 2. Figure 3 presents the solution of the inverse kinematics in the joint-space, the results show that all the solutions for all the poses exhibit a variability produced by the uncertain lengths of the non-dimensional links.

The results of Table 3 indicate a similar behavior of the variability of the inverse kinematics when compared to the forward kinematics of Table 2. The variability of the inverse kinematics depends on the specific pose where the model is evaluated, i.e., the variability increases at poses closed to singular loci and also for the outer limits of workspace.

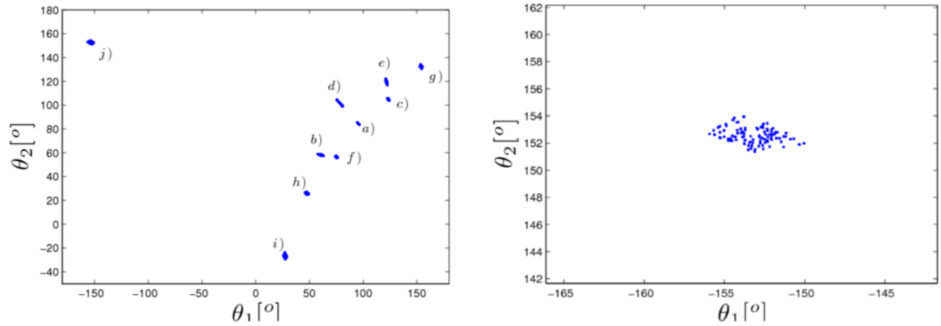

(a) (b)

Figure 3. Inverse Kinematic solutions with uncertain parameters: (a) For all cases, (b) Case j).

3.3. Workspace

The usable workspace and MIW are also determined as function of the uncertain non-dimensional lengths of the links $r_1(\Omega)$, $r_2(\Omega)$ and $r_3(\Omega)$ presented in Table. 1. Based on

Table 3. Inverse Kinematic with Uncertainties.

Case	x	y	$\overline{\theta_1}$	$\overline{\theta_2}$	σ_{θ_1}	σ_{θ_2}
a)	0.0000	1.5970	95.5153	84.4847	0.3793	0.3793
b)	0.6200	1.5970	60.8415	58.0334	0.9729	0.3349
c)	-0.6200	1.5970	121.9666	119.1585	0.3349	0.9729
d)	0	2	78.8325	101.1675	1.1005	1.1005
e)	-0.5000	1.2700	123.5343	104.7780	0.3886	0.4019
f)	0.5000	1.2700	75.2220	56.4657	0.4019	0.3886
g)	-1	1	154.1027	132.2211	0.4888	0.6565
h)	1	1	47.7789	25.8973	0.6565	0.4888
i)	1.2000	0.2000	27.4687	-26.8207	0.5524	1.2538
j)	-1.2000	0.2000	-153.1793	152.5313	1.2538	0.5524

Eq. (19), the MIW with the uncertain parameters can be obtained by using the follow expression:

$$[r_{MIW}(\Omega) y_{MIW}(\Omega)] = g\big(r_1(\Omega), r_2(\Omega), r_3(\Omega)\big) \tag{23}$$

As presented in Fig. 4, the uncertainties in the non-dimensional lengths introduce an small variability in the shape of the usable workspace and the MIW, i.e., the Fig. 4 shows the plotting of all the possible realizations of the workspace with the uncertain parameters, for this reason there is an increment in the thickness of the limits of usable workspace and MIW.

The variability of the MIW is presented in Table 4. It is also observed that the uncertain parameters introduce a variability in the center and radius of the MIC, this could produce also a variability in the kinematic performance of the 5R symmetric mechanism, specifically in the Global Condition Index that is evaluated over the MIW [9].

4. Conclusions

This paper presents a methodology to evaluate the kinematic performance of the planar 5R parallel mechanism with uncertainties by using a stochastic analysis. The uncertain were considered in the non-dimensional length of the links and the clearances of the active joints, these uncertain parameters were modeled as random variables. The forward kinematics, inverse kinematic and workspace were evaluated by using the Monte Carlo Simulation.

Simulation results indicated a non-negligible variability in the kinematic model of the mechanism. Consequently, the effects produced by the uncertainties should be taken into account in order to design parallel mechanism subjected to uncertainties.

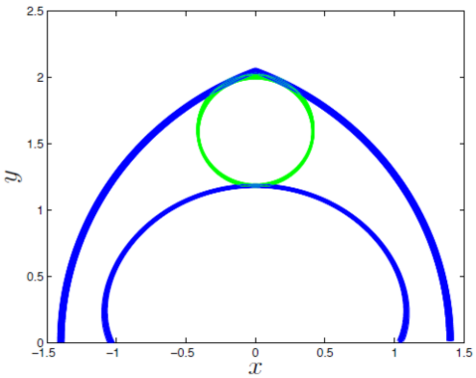

Figure 4. Usable and Maximum Inscribed Workspace with uncertainties.

Table 4. Maximum Inscribed Workspace with Uncertainties

$\bar{r}_{MIW}$	$\bar{y}_{MIW}$	$\sigma_{r_{MIW}}$	$\sigma_{y_{MIW}}$
0.4138	1.5970	0.0041	0.0085

Acknowledgement

The authors express their acknowledgements to the Graduate Program of Mechanical Engineering of the Federal University of Technology - Paraná funded by CAPES.

References

[1] F. A. Lara-Molina, E. H. Koroishi, D. Dumur, V. Steffen Jr., Stochastic Analysis of a 6-DOF Fully Parallel Robot under Uncertain Parameters, *IFAC-PapersOnLine,* Vol. 48, 2015, No. 19, pp. 214–219.

[2] S. Rao, P. Bhatti, Probabilistic approach to manipulator kinematics and dynamics, *Reliability Engineering and System Safety*, Vol. 72, 2001, pp. 4–58.

[3] M. D. Pandey, X. Zhang, System reliability analysis of the robotic manipulator with random joint clearances, *Mechanism and Machine Theory*, Vol. 58**,** 2012, pp. 137–152.
[4] X-J. Liu, J. Wang, G. Pritschow, Performance atlases and optimum design of planar 5R symmetrical parallel mechanism, *Mechanism and Machine Theory*, Vol. 41**,** 2006, No. 2, pp. 119–144.
[5] P. Voglewede, A.H.C. Smith, A. Monti, Dynamic performance of a scara robot manipulator with uncertainty using polynomial chaos theory, *IEEE Transactions on Robotics*, Vol. 25, 2009, No. **1,** pp. 206–210.
[6] F.A. Lara-Molina, E.H. Koroishi, V. Steffen, Uncertainty analysis of a two-link robot manipulator under fuzzy parameters, *Robotics: SBR-LARS Robotics Symposium and Robocontrol (SBR LARS Robocontrol),2014 Joint Conference on,* 2014, pp. 1–6.
[7] F. A. Lara-Molina, J. M. Rosario, D. Dumur, P. Wenger, Generalized Predictive Control of Parallel Robots, *Robot Motion and Control 2011*, 2012, pp. 159–169.
[8] A. Florian, An efficient sampling scheme: updated latin hypercube sampling, *Probabilistic engineering mechanics*, Vol. 7, 1992, No. 2, pp. 123–130.
[9] X-J. Liu, J. Wang, G. Pritschow, Kinematics, singularity and workspace of planar 5R symmetrical parallel mechanisms, *Mechanism and Machine Theory*, Vol. 41, 2006, No. 2, pp. 145–169.